

an and J. L. Peube (Gordon and Breach, London, 1977), p. 235.

⁵S. A. Orszag, in *Computing Methods in Applied Sciences and Engineering*, edited by R. Glowinski and J. L. Lions (Springer, Berlin, 1974), Pt. 2, p. 50.

⁶A. Brissaud, U. Frisch, J. Leorat, M. Lesieur, A. Mazure, A. Pouquet, R. Sadourny, and P. L. Sulem, *Ann. Geophys.* **29**, 539 (1973).

⁷G. I. Taylor and A. E. Green, *Proc. Roy. Soc. London, Ser. A* **158**, 499 (1937).

⁸D. S. Gaunt and A. J. Guttman, in *Phase Transitions and Critical Phenomena*, edited by C. Domb and M. S. Green (Academic, London, 1974), Vol. 3, p. 181. Also, G. S. Rushbrooke, G. A. Baker, Jr., and P. J. Wood, *ibid.*, p. 246.

⁹These initial conditions are analytic in \vec{x} , so the flow remains so for at least a finite time. See C. Bardos, *C. R. Acad. Sci. (Paris)* **283A**, 255 (1976).

¹⁰With the initial conditions (2)–(4), the fact that the series for $\Omega_p(t)$ involves only even powers of t follows from invariance under time reversal.

¹¹M. D. Van Dyke, *SIAM J. Appl. Math.* **28**, 720 (1975). Also, R. J. Fateman and S. A. Orszag (unpublished) used the algebraic manipulation program MACSYMA to compute $\Omega_1(t)$ to order t^{10} analytically.

¹²Even utilizing all the many symmetries (see Ref. 5) of the flow, the computation of Ω_p to order t^{44} with 29-digit precision required about 7 h on a CDC 7600 computer. Since the required work to calculate to order t^n scales as n^8 , further computations are very costly. An alternative computational procedure is to use transform methods (see Ref. 5) to evaluate the nonlinear term in (1), which requires order $n^5 \ln n$ operations. Never-

theless, the code based on the present method is more efficient through order t^{50} because not all modes are excited at once.

¹³The error estimate is inferred from a comparison of the present double-precision results with single-precision calculations to order t^{28} . At order t^{28} , absolute errors in the single-precision results are about 10^{-14} , so that single-precision results lose all significance beyond order t^{30} . On this basis, we assume that the absolute errors in the double-precision results at order t^{44} are about 10^{-27} .

¹⁴Padé approximations to $d \ln \tilde{\Omega}_k / d w$ also show a real singularity at $t_* \approx 5.2$ with a residue $-\gamma_1 \approx -0.8$.

¹⁵U. Frisch and R. H. Morf, unpublished. They analyze the solutions to a nonlinear Langevin equation in time t with band-limited forcing and find that small-scale structure is intimately related to the distribution of singularities in the complex t plane.

¹⁶The critical exponents γ_p do not appear to lie in arithmetic progression. Thus, it seems that more than one significant length scale is responsible for flow breakdown near t_* .

¹⁷More recent studies of Ω_p with noninteger p (done with D. Meiron) suggest the preliminary result that a singularity appears at t_* for $p \gtrsim 0.3$. Further work is now underway to substantiate this result and its possible connection with the inertial-range turbulence spectrum. We remark that Ω_p is singular for $p \geq 1/3$ if the Kolmogorov $k^{-5/3}$ spectrum is established.

¹⁸S. A. Orszag and C. M. Tang, *J. Fluid Mech.* **90**, 129 (1979).

¹⁹D. W. Moore, *Proc. Roy. Soc. London, Ser. A* **365**, 105 (1979).

Nonlinear Inverse Bremsstrahlung and Heated-Electron Distributions

A. Bruce Langdon

Lawrence Livermore Laboratory, University of California, Livermore, California 94550

(Received 25 May 1979)

When $Zv_0^2/v_e^2 \gtrsim 1$, inverse bremsstrahlung results in a non-Maxwellian velocity distribution for which the absorption is reduced by up to a factor of 2 compared with the Maxwellian distribution usually assumed. Transport and atomic processes are also altered. Especially in materials with $Z \gg 1$, this is significant at lower intensities than for the well-known nonlinearity for which the measure is v_0^2/v_e^2 .

Light absorption by inverse bremsstrahlung remains attractive in laser-induced fusion schemes, as compared with absorption by collective processes which heat a minority of the electrons to superthermal energies. These electrons preheat the target core and do not effectively drive an ablative implosion. To make inverse bremsstrahlung competitive it may require that the ion charge state Z greatly exceed 1. Especially in this case, but also for $Z = 1$, I will demonstrate

nonlinear modifications which take effect at lower intensities than the absorption nonlinearity analyzed many times before.¹⁻⁴ A second refinement removes the usual restriction that the light frequency must greatly exceed the collision frequency.

We reexamine the collisional absorption (inverse bremsstrahlung) of intense laser light in a dense plasma, considering heating and diffusion of electrons of various energies, the evolu-

tion to a non-Maxwellian electron distribution when $Zv_0^2/v_e^2 \geq 1$, and the resulting changes to transport and other properties. [Here v_0 is the peak velocity of oscillation of the electrons in the high-frequency electric field, $v_e \equiv (T_e/m_e)^{1/2}$ is the electron thermal velocity, and Z is the ionization state.] For example, the absorption itself can be reduced by a factor of 2 compared with the absorption in a Maxwellian plasma of the same thermal energy density. For materials with $Z \gg 1$, this is significant at lower intensities than required by the more familiar nonlinearity for which the relevant parameter is v_0^2/v_e^2 . This ratio may be expressed as $v_0^2/v_e^2 = 4 \times 10^{-16} I \lambda^2 / T_e$, where I is the intensity in W/cm^2 , λ is the vacuum wavelength in micrometers and T_e is the electron temperature in kiloelectronvolts.

The origin of this nonlinearity is that, when $Zv_0^2/v_e^2 \geq 1$, electron-electron ($e-e$) collisions are not rapid enough to make the flat-topped velocity distribution produced by inverse bremsstrahlung Maxwellian. As a clue to this result, consider the ratio of the e -folding time for heating to the $e-e$ equilibration time τ_{ee} required to reestablish a Maxwellian distribution. For a Maxwellian distribution, the heating time is (thermal energy)/ $\vec{J} \cdot \vec{E} = 3\tau_e v_e^2 / v_0^2$. We have expressed the absorption^{2,5} in terms of v_0 and $\tau_e^{-1} = [4(2\pi)^{1/2}/3] n_e Z e^4 \ln \Lambda / m_e^2 v_e^3$, the same as the standard Maxwell-weighted $e-i$ scattering rate^{6,7} (except for a small modification⁵ to $\ln \Lambda$). The heating time is shorter than τ_{ee} ($\cong \tau_e/Z$) when $Zv_0^2/v_e^2 \geq 3$, in which case non-Maxwellian distributions are possible.

In computer modeling of experiments in which inverse bremsstrahlung is thought to be the dominant absorption mechanism, agreement with experiment often requires invoking mechanisms which reduce absorption. Perhaps the effect described here has such a role in the experiments of Shay *et al.*⁸ There, with intensities of $\sim 10^{14}$ W/cm^2 at wavelength $1.06 \mu\text{m}$, electron temperatures of ~ 400 eV and $Z \sim 10$ ("a conservative choice tending not to overestimate absorption"), I find $v_0^2/v_e^2 \cong 0.1$, and so the conventional nonlinearity¹⁻⁴ makes only a 1.5% reduction in opacity. However, since $Zv_0^2/v_e^2 \cong 1$, the nonlinearity described here results in a 40% reduction, comparable to other refinements invoked in Ref. 8 to improve agreement with experiment.

The nonlinearity of Refs. 1-4,⁴ for which the measure is v_0^2/v_e^2 , arises as follows: In the standard treatment, a Maxwellian electron distribution oscillates relative to the ions. The

drag on an isotropic distribution shifted by V is⁹ $\propto V^{-2}$ (fraction of the electrons for which $|v-V| < V$). This is linear for small V/v_e but increases more slowly at larger V/v_e , finally decreasing $\propto V^{-2}$. It may seem that only electrons whose thermal velocities are less than the drift V contribute to the absorption.² In fact, some of the faster electrons *do* gain energy while others lose in such a way that no net energy is lost from the field to these electrons. This diffusion and velocity dependence of the absorption are clarified below.

I derive the equation of evolution of the electron distribution function f due to $e-i$ scattering in the presence of an oscillating electric field. For $h\nu \ll T_e$, there is good agreement between quantum and classical descriptions^{2,4} except for modifications to $\ln \Lambda$, and so I use a simple classical model^{3,7} for clarity. If one assumes uniform density and field, the kinetic equation is

$$\frac{\partial f}{\partial t} - \frac{e}{m_e} \vec{E} \cdot \frac{\partial f}{\partial \vec{v}} = A \frac{\partial}{\partial \vec{v}} \cdot \left[\frac{v^2 \vec{I} - \vec{v}\vec{v}}{v^3} \cdot \frac{\partial f}{\partial \vec{v}} \right] + C_{ee}(f), \quad (1)$$

with $A = (2\pi m_e Z e^4 / m_e^2) \ln \Lambda$, in the usual notation. C_{ee} is the $e-e$ collision operator. Expansion in Legendre functions, $f(\vec{v}, t) = \sum f_1(v, t) P_1(\mu)$, simplifies the $e-i$ collision operator. The first two equations are⁷

$$\frac{\partial f_0}{\partial t} - \frac{eE}{m_e} \frac{1}{3v^2} \frac{\partial}{\partial v} (v^2 f_1) = C_0, \quad (2)$$

$$\begin{aligned} \frac{\partial f_1}{\partial t} - \frac{eE}{m_e} \left(\frac{\partial f_0}{\partial v} + \frac{2}{5v^3} \frac{\partial}{\partial v} (v^3 f_2) \right) \\ = - \frac{2A}{v^3} f_1 + C_1, \end{aligned} \quad (3)$$

with $eE(t)/m\omega = v_0 \cos \omega t$. I have truncated the expansion by neglecting f_2 ; this implies $v_0^2/v_e^2 \ll 1$. The effects of $v_0^2 > v_e^2$ for a Maxwellian distribution have been discussed extensively,¹⁻⁴ whereas my present purpose is to demonstrate that such modifications are possible even when $v_0^2 \ll v_e^2$, so that one may be allowed to make this simplification.

At such intensities, the time dependence of f_1 is predominantly at the high-frequency ω and it is the slow variation of f_0 which is relevant. C_0 is evaluated using only f_0 [Eq. (7-71b), Ref. 7]. As $e-e$ collisions do not much affect the oscillating flux f_1 , except indirectly through the slow

variation of f_0 , I drop C_1 . I obtain

$$\begin{aligned} \langle \vec{E} \cdot \vec{J} \rangle &= -\frac{4\pi}{3} A n_e m_e v_0^2 \int_0^\infty dv g \frac{\partial f_0}{\partial v} \\ &= \frac{4}{3} \pi A n_e m_e v_0^2 \int_0^\infty dv \frac{\partial g}{\partial v} f_0, \end{aligned} \quad (4)$$

$$\frac{\partial f_0}{\partial t} = \frac{A v_0^2}{3} \frac{1}{v^2} \frac{\partial}{\partial v} \left(\frac{g}{v} \frac{\partial f_0}{\partial v} \right) + C_0(f_0), \quad (5)$$

with $g(v) = [1 + \omega^{-2} \tau_{ei}^{-2}(v)]^{-1} (1 + v \omega^6 / v_0^6)^{-1}$, where $\tau_{ei}^{-1}(v) \equiv 2A/v^3$ is the electron scattering rate and v_ω is defined by $\omega \tau_{ei}(v_\omega) = 1$. The rate of change of kinetic energy calculated from Eq. (5) is consistent with the absorption, Eq. (4).

The function g accounts for the changeover from the primarily *reactive* response of the faster electrons to *resistive* response of the slow, strongly scattered electrons. Usually, collisions are treated as a perturbation on the oscillation of the *entire* distribution,¹⁻⁵ i.e., $\omega \tau_{ei} \gg 1$ for *all* electrons; so that $g \equiv 1$ and, from Eq. (5), absorption is⁷ $\propto f_0(v=0)$ for $v_0/v_e \rightarrow 0$. For Maxwellian f_0 , this leads to the standard linear absorption result.^{1,2,5,7} Here, one sees that absorption is $\propto f_0$ evaluated, where g increases rapidly from ≈ 0 to ≈ 1 , i.e., at the velocity v_ω for which scattering and light frequencies are matched, $\omega \tau_{ei}(v_\omega) \approx 1$. Numerical evaluation of Eq. (4) shows that absorption is reduced by a factor given within 3% by $\exp(-v_\omega^2/2v_e^2)$, for $v_\omega \leq 2v_e$. Electrons with velocity v_ω have energy $8[(n/n_c)(Z/\lambda) \ln \Lambda/10]^{2/3}$ eV, where n_c is the critical density for the light, which has vacuum wavelength λ in micrometers. Although this energy can be several hundred electron volts, unless T_e is much higher than this, the opacity is so large that the laser light may have been entirely absorbed at lower densities. The opacity is² $\kappa = (n/n_c)/c\tau_e$; if $v_\omega = v_e$ then $\omega \tau_e = 3(\pi/2)^{1/2}$ and $\kappa \lambda \equiv 2\pi c \kappa / \omega = 1.7 n/n_c$, so that light is mostly absorbed in $\sim n_c/n$ wavelengths.

Numerical solutions illustrate the evolution of f_0 and its effect on absorption and other macroscopic properties. I use a numerical scheme similar to one in Killeen, Mirin, and Rensink,¹⁰ in which the Fokker-Planck coefficients are calculated from f_0 without linearization, except that the energy consistency between the finite difference forms of Eqs. (4) and (5) is preserved, and the rapidly decreasing "tail" of the distribution is correctly represented (at least in thermal equilibrium); both properties are independent of the spacing of the velocity zones, which are lar-

ger at higher velocities.

I consider first the effect of inverse bremsstrahlung alone, corresponding to the limit $Zv_0^2/v_e^2 \gg 1$. An initially monoenergetic distribution diffuses and slows in balance so that no net gain in kinetic energy results, Fig. 1, curve *a*. When electrons reach low velocities [such that $\omega \tau_{ei}(v) \leq 1$] their loss of energy is slowed while upward diffusion of faster particles continues, so net absorption begins. This is the meaning of the result that the absorption depends on f_e at $v \approx v_\omega$. By the time the electrons have gained only 10% in energy (Fig. 1, curve *b*), f_0 is close to its late-time form, described by a similarity solution of the form¹¹ $u^{-3} \exp(-v^5/5u^3)$, with $u^5 = 5Av_0^2t/6$, which is derived from Eq. (5) with $g \equiv 1$. For this distribution, the absorption is only 45% of what it would be if electron-electron collisions enforced a Maxwellian distribution.

We now argue that it is possible for *e-e* collisions to be the other principal influence on f_0 ,

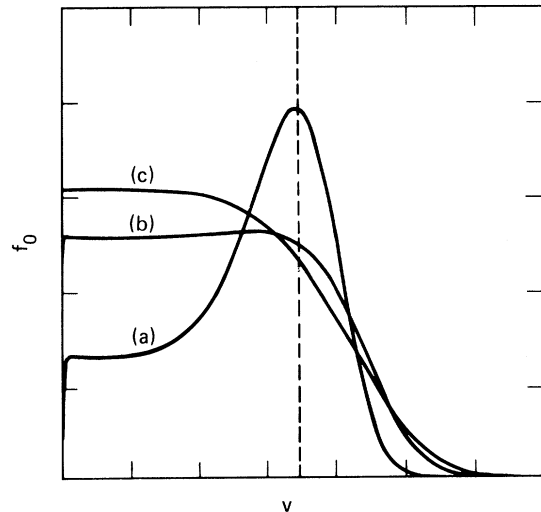


FIG. 1. Evolution of an initially monoenergetic distribution f_0 due to *e-i* collisions in the presence of an oscillating field; *e-e* collisions are neglected corresponding to large Zv_0^2/v_e^2 . The initial velocity, indicated by the dashed line, is $5.8v_\omega$. At first, electrons diffuse both up and down in balance so that f_0 evolves greatly before it gains only 1% in energy, curve *a*. Thereafter, the slowest electrons cannot lose more energy, while others continue to diffuse upward, resulting in net absorption. When the energy has increased by 10%, curve *b*, f_0 is close to the self-similar solution curve *c*, which is normalized to the same energy as curve *b*. Both axes are linear. A change in initial velocity, or in the constant A , scales the times corresponding to curves *a-c* but does not alter their shape.

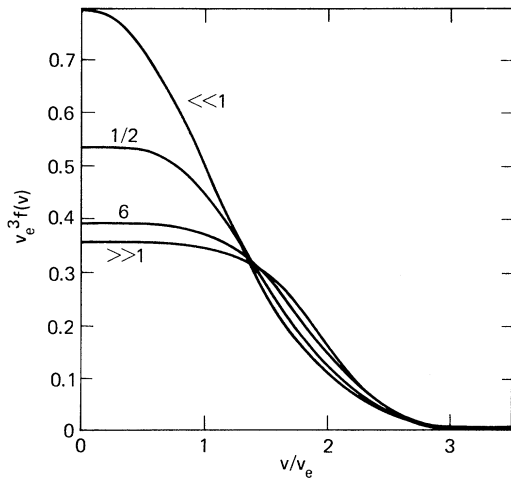


FIG. 2. Distributions corresponding to various values of Zv_0^2/v_e^2 , where $v_e^2 \equiv \langle v^2 \rangle / 3$. These are of course not steady state, but are distributions plotted when Zv_0^2/v_e^2 decreases through specified values as the plasma heats up from a much lower temperature. $Zv_0^2/v_e^2 \gg 1$ corresponds to the self-similar solution, and $Zv_0^2/v_e^2 \ll 1$ is Maxwellian.

in addition to inverse bremsstrahlung. First note that $\kappa\lambda_{\text{mfp}} = \kappa v_e \tau_e = (v_e/c)(n/n_c) \ll 1$, i.e., the optical depth is many mean free paths deep. If one assumes a large temperature gradient $\sim \kappa$, as if the gradient is due to nonuniform absorption, heat flow cannot greatly change the distribution more quickly than a thermal electron can diffuse across the distance κ^{-1} ; this transit time is $\sim \tau_e / (\kappa\lambda_{\text{mfp}})^2$. Thus $\tau_{ee} / (\text{transit time}) \cong Z(v_e/c)^2 (n/n_c)^2$. This ratio will often be < 1 , so that e - e collisions would take effect more rapidly than heat flow.¹² (In fact, transport theory^{6,7} relies on e - e collisions maintaining a near Maxwellian.) This estimate is weakest when applied to superthermals. In any case, heat flow does not replenish the slowest particles and therefore affects absorption very little.

For $\alpha = Zv_0^2/v_e^2 \geq 1$, electron-electron collisions alter the results only slightly. For example, with $\alpha = 6$ the absorption is still only 49% of its Maxwellian value, and inverse bremsstrahlung contributes equally with electron-electron collisions to diffusion of superthermals into the "tail" of the distribution. With $\alpha = 0.5$, the distribution is still depressed and flattened near $v = 0$ (Fig. 2), and absorption is reduced to 67% of normal. When α is only 0.05 the reduction is 12%. For any α , the reduction factor is $1 - 0.553/[1 + (0.27/\alpha)^{0.75}]$ within ± 0.005 ; see also Fig. 3.

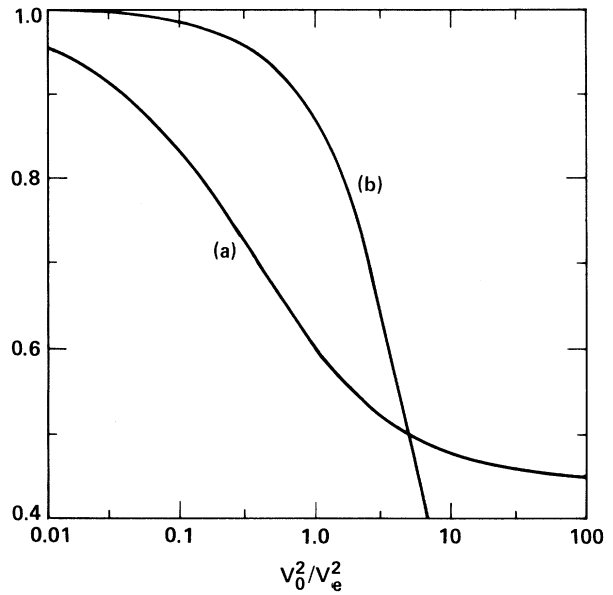


FIG. 3. Comparison of reduction in opacity by the nonlinear mechanisms of this paper (curve *a*) and of Refs. 1-4 (curve *b*). The abscissa of curve *b* is normalized to correspond to curve *a* for $Z=1$ and equal light intensity in circular polarization. If $Z > 1$, curve *b* would remain closer to 1. Thus, for any Z and $v_0^2/v_e^2 \lesssim 1$, the mechanism of this paper dominates.

Full quantitative evaluation of this effect requires incorporation of spatial gradients and transport. In turn, the transport itself, and the degree of ionization Z , are themselves affected by these distributions. Heat conductivity and collisional ionization are determined mainly by the tail of the distribution, which is truncated here. On the other hand, atomic recombination is effected by the slow electrons where our distributions are also deficient compared with a Maxwellian. Enhanced ion fluctuations (above thermal level) act similarly to the high- Z situation in increasing the absorption rate¹³ relative to the e - e collision rate; therefore non-Maxwellian distributions again result, although with a different dependence than discussed here. Finally, we note that the nonlinear results in Refs. 1-4 appear not to be applicable at *any* intensity of Z , because, with $v_0^2/v_e^2 \lesssim 1$, we find a much larger effect than they do, while for $v_0^2/v_e^2 \geq 1$ the oscillating electron distribution is not even isotropic, much less Maxwellian as they assume. A correct treatment of this situation remains to be done.

It is a pleasure to acknowledge valuable conversations with W. I. Kruer, G. B. Zimmerman,

and C. E. Max. This work was performed under the auspices of the U. S. Department of Energy, at the Lawrence Livermore Laboratory under Contract No. W-7405-Eng-48.

¹V. P. Silin, Zh. Eksp. Teor. Fiz. 47, 2254 (1964) [Sov. Phys. JETP 20, 1510 (1965)].

²R. E. Kidder, in *Physics of High Energy Density*, edited by P. Caldirola and H. Knoepfel (Academic, New York, 1971), p. 306.

³P. J. Catto and T. Speziale, Phys. Fluids 20, 167 (1977).

⁴For recent results and listings of earlier work see Y. Shima and H. Yatom, Phys. Rev. A 12, 2106 (1975); H. Brysk, J. Phys. A 8, 1260 (1975); L. Schlessinger and J. Wright, Phys. Rev. A 20, 1934 (1979).

⁵J. Dawson and C. Oberman, Phys. Fluids 5, 517 (1962); T. W. Johnston and J. M. Dawson, Phys. Fluids 16, 722 (1973).

⁶S. I. Braginskii, in *Reviews of Plasma Physics*, ed-

ited by M. A. Leontovich (Consultants Bureau, New York, 1965), Vol. 1, p. 205.

⁷I. P. Shkarofsky, T. W. Johnston, and M. P. Bachynski, *The Particle Kinetics of Plasmas* (Addison-Wesley, Reading, Mass. 1966).

⁸H. D. Shay, R. A. Haas, and W. L. Kruer *et al.*, Phys. Fluids 21, 1634 (1978).

⁹B. A. Trubnikov, in *Reviews of Plasma Physics*, edited by M. A. Leontovich (Consultants Bureau, New York, 1965), Vol. 1, p. 174.

¹⁰J. Killeen, A. A. Mirin, and M. E. Rensink, in *Methods in Computational Physics*, edited by J. Killeen (Academic, New York, 1976), Vol. 16, p. 389.

¹¹The same velocity dependence arises in electron heating by ion waves with an isotropic spectrum, as shown in the two-dimensional case by R. Z. Sagdeev and A. A. Galeev, in *Nonlinear Plasma Theory* (Benjamin, New York, 1969), Chap. 2.

¹²On the other hand, electrons quickly cross the intensity modulations in a standing wave, so that one should then use simply the spatial average of v_0^2 .

¹³J. Dawson and C. Oberman, Phys. Fluids 6, 394 (1963).

Spatially Resolved Suprathermal X-Ray Emission from Laser-Fusion Targets

N. M. Ceglio and J. T. Larsen

Lawrence Livermore Laboratory, University of California, Livermore, California 94550

(Received 29 October 1979)

High-resolution images of suprathermal x-ray emission from laser-imploded fusion targets have been recorded. The images show the spatial distribution of the relatively cold pusher material during the early stages of target implosion. There is evidence of an early, asymmetric breakup of the pusher shell.

X-ray emission spectra from laser-driven fusion targets commonly exhibit a suprathermal x-ray (STX) component.¹ The STX's are bremsstrahlung produced by radiative interactions between suprathermal electrons (STE's) and background plasma ions, and as such are characteristic of a significant STE population. The physical mechanisms governing the production and transport of STE's are vital to an understanding of laser-driven implosions. Images of the STX emission can provide insight into these mechanisms.

This Letter reports the first high-resolution images of the suprathermal x-ray emission from laser-driven fusion targets. The images (1) show the distribution of the relatively cold pusher material during target irradiation, (2) provide evidence of breakup of the pusher during the early stages of implosion, and (3) illustrate spatial inhomogeneities in suprathermal electron produc-

tion.

The STX imaging experiments were conducted using the Shiva laser-target irradiation facility at Lawrence Livermore Laboratory. This laser system produces a twenty-beam, multiterawatt pulse of 1.06- μm radiation. Typical pulse duration for these experiments was 90 psec, with 17–20 TW delivered to the target. The twenty beams were focused onto the target in two opposing ten-beam clusters. The typical target was a spherical glass microshell (o.d. $\sim 300\text{--}325\ \mu\text{m}$; wall thickness $\sim 1.5\text{--}2.0\ \mu\text{m}$) with an equimolar DT gas fill $\sim 2\ \text{mg}/\text{cm}^3$. Typical target yield was $(0.5\text{--}1.0) \times 10^{10}$ neutrons.

High-resolution, time-integrated images of the STX emission from these exploding pusher targets were obtained using a coded imaging technique, zone-plate coded imaging.^{2,3} The zone-plate camera subtended a solid angle $\sim 4 \times 10^{-2}$ sr, had a 3-cm target-to-zone-plate distance,